Adaptive, nonlinear state transformation-based control of motion in presence of hard constraints

J. KABZIŃSKI* and P. MOSIOŁEK

Institute of Automatic Control, Lodz University of Technology, Stefanowskiego 18/22 Lodz, Poland

Abstract. The paper describes a nonlinear controller design technique applied to a servo drive in the presence of hard state constraints. The approach presented is based on nonlinear state-space transformation and adaptive backstepping. It allows us to impose hard constraints on the state variables directly and to achieve asymptotic tracking of any reference trajectory inside the constraints, despite unknown plant parameters. Two control schemes (with and without integral action) are derived, investigated and then compared. Several examples demonstrate the main features of the design procedure and prove that it may be applied in case of motion control problems in electric drive automation.

Key words: motion control, nonlinear control, adaptive control, state constraints.

1. Introduction

High-precision motion control remains the fundamental problem of control theory and numerous applications. Robotics (mobile robots and industrial manipulators) is a typical application area, but the same problems and solutions appear in a wide variety of high-performance mechatronic systems, including micro- and nanoscale motion, machine and CNC tools, manufacturing tools, numerous servo drives, etc. The main factors influencing control performance and quality are the unknown parameters of the plant model and the nonlinear nature of load or disturbing torques. Therefore, adaptive nonlinear control techniques are widely and successfully applied in motion control problems.

All practical systems are influenced by a variety of constraints. In a servo drive both main state variables – position and speed – are bounded. Very often, the constraints are "hard", i.e. any, even a small violation is unacceptable as it may cause mechanical damage of the machine or its surroundings, or even contrive a danger for human users. Therefore, nonlinear, adaptive control in the presence of hard state constraints remains an important issue. Some powerful control techniques have been developed to deal with this problem. Methods based on set invariance [1], admissible set control [2, 3], model predictive control [4, 5] and reference governors [6, 7] produce numerical algorithms with a heavy computation burden and now mostly bear historical importance. Recently, the barrier Lyapunov functions (BLF) approach was used to cope with various (state [8, 9] or output [10, 11], constant or varying [12, 13]) constraints, also for motion control [14, 15]. But, the BLF approach

to the tracking problem allows for imposing constraints for the error system merely and the effective constraints for state variables must be derived taking into account the reference trajectory and the controller parameters used in subsequent control loops. The controller obtained is applicable only If it is possible to find a set of design parameters that satisfies the so-called "feasibility conditions" [16, 17].

In this contribution, we propose a new approach to nonlinear, adaptive motion control in the presence of hard state constraints based on nonlinear state-space transformation. This allows us to impose hard constraints on the state variables directly and to achieve asymptotic tracking of any reference trajectory inside the constraints, in spite of the plant parameters remaining unknown. The paper finds its place in the important area of adaptive control applications to motion control problems. Adaptive techniques are used in [18, 19] for tracking control and in [20, 21] for state observation. The proposed approach to handling hard state constraints is a new contribution.

2. Plant model and control objectives

The drive under consideration is modelled by two differential equations:

$$\begin{aligned}
\dot{x}_1 &= x_2, \\
J\dot{x}_2 &= \theta^T \xi(x_1, x_2, t) + gu.
\end{aligned} \tag{1}$$

The angular or linear position is denoted by x_1, the rotational or linear speed by x_2, J corresponds to system inertia while $g > 0$ represents the transformation of the control input u into the propulsion torque or force. Component $f = \theta^T \xi(x_1, x_2, t)$ describes all load or disturbance torques/forces such as friction, torque/force ripples, etc. Function ξ is known. Unknown, constant parameters in p-dimensional vector θ will be approxi-

mated by the adaptive parameters. It is assumed that parameters J and g are also unknown, although they remain positive and constant.

This type of equation may be used to model rotational or linear motion of numerous plants with a different source of propulsion. If an electric (rotational or linear) drive with a DC or a synchronous permanent magnet motor is considered, model (1) is obtained under the assumption that the current control loop is much faster than the mechanical dynamics. The model of a robotic manipulator with multiple joints is a straightforward generalization of (1) – in this case, f includes centripetal-Coriolis forces, gravitational forces and frictional as well as disturbing forces. The same structure of the model may also be proposed for pneumatic servo systems.

Hard, asymmetric constraints are considered for both state variables:

$$-b_{i,1} < x_i < b_{i,2}, \qquad i = 1, 2. \tag{2}$$

The control aim is to follow the desired, smooth trajectory x_{1d}, $\dot{x}_{1d}$ with sufficient accuracy under the inviolable constraints (2).

3. Nonlinear state transformation

New state variables are introduced:

$$s_i = \ln \frac{b_{i,1} + x_i}{b_{i,2} - x_i}, \qquad i = 1, 2. \tag{3}$$

The new state variable $s_i \to -\infty$ if $x_i \to -b_{i,1}$ and $s_i \to \infty$ if $x_i \to b_{i,2}$. Therefore, singularities in (3) correspond to bounds imposed on state variables x_i. The transformation defined in (3) is a bijection between the open set (2) and the real axis and the inverse is given by:

$$x_i = b_{i,2} - \frac{b_{i,2} + b_{i,1}}{e^{s_i} + 1} = -b_{i,1} + \frac{(b_{i,2} + b_{i,1})}{e^{-s_i} + 1}. \tag{4}$$

Equations describing the dynamics of new state variables are as follows:

$$\dot{s}_i = \frac{\mathrm{d}}{\mathrm{d}t} \ln \frac{b_{i,1} + x_i}{b_{i,2} - x_i} = \frac{2 + e^{-s_i} + e^{s_i}}{b_{i,2} + b_{i,1}} \dot{x}_i =: k_i(s_i)\dot{x}_i. \tag{5}$$

Functions $k_i(s_i)$ are nonzero for any $-\infty < s_i < \infty$:

$$|k_i(s_i)| = \left| \frac{2 + e^{-s_i} + e^{s_i}}{b_{i,2} + b_{i,1}} \right| \geq \frac{4}{|b_{i,2} + b_{i,1}|}. \tag{6}$$

Derivatives of $k_i(s_i)$

$$h_i(s_i) := \frac{\mathrm{d}}{\mathrm{d}s_i} k_i(s_i) = \frac{-e^{-s_i} + e^{s_i}}{b_{i,2} + b_{i,1}}, \tag{7}$$

$$\frac{\mathrm{d}}{\mathrm{d}t} k_i(s_i) = h_i(s_i)\dot{s}_i = h_i(s_i)k_i(s_i)\dot{x}_i \tag{8}$$

are available for the controller design.

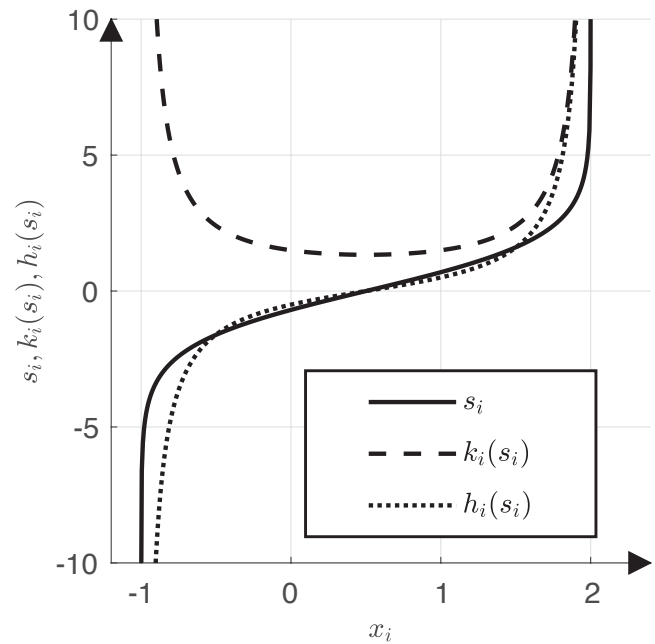Typical behavior of the functions describing the proposed transformation is illustrated in Fig. 1.

Fig. 1. Plots of s_i, $k_i(s_i)$, $h_i(s_i)$ for $-b_{i,1} = -1$, $b_{i,2} = 2$

A similar transformation is applied to the reference trajectory, leading to:

$$s_{1d} := \ln \frac{b_{1,1} + x_{1d}}{b_{1,2} - x_{1d}}, \qquad \dot{s}_{1d} = k_1(s_{1d})\dot{x}_{1d}. \tag{9}$$

4. Controller design

The adaptive controller is designed using the backstepping approach [22, 23]. It is based on the error system defined in the transformed state-space. For application purposes, it is enough to prove the uniform, ultimate boundedness (UUB) [24] of errors and the boundedness of transformed state variables s_i.

The tracking error is defined for the variables being transformed:

$$\begin{aligned} \varepsilon_1 &:= s_{1d} - s_1, \\ \dot{\varepsilon}_1 &= k_1(s_{1d})\dot{x}_{1d} - k_1(s_1)\dot{x}_1. \end{aligned} \tag{10}$$

Step 0:

The additional integral action is added to the standard backstepping design. Therefore, the error integral is considered at the initial stage of backstepping:

$$p := \int_0^t \varepsilon_1(\tau)\,\mathrm{d}\tau. \tag{11}$$

The trajectory of p is described by:

$$\dot{p} = \varepsilon_1. \tag{12}$$

If signal ε_1 is forced to follow the desired trajectory:

$$\varepsilon_{1d} = -L_0 p, \qquad L_0 > 0, \qquad \varepsilon_0 := \varepsilon_1 - \varepsilon_{1d}, \qquad (13)$$

where $L_0 > 0$ is a design parameter, system (12) is stable for $\varepsilon_0 \to 0$, as it follows from the Lyapunov function:

$$V_0 = \frac{1}{2} p^2 \Rightarrow \dot{V}_0 = -L_0 p^2 + p \varepsilon_0. \qquad (14)$$

Step 1:

At the next stage of the design, the trajectory of ε_0 is considered:

$$\dot{\varepsilon}_0 = \dot{\varepsilon}_1 - \dot{\varepsilon}_{1d} = k_1(s_{1d})\dot{x}_{1d} - k_1(s_1)\dot{x}_1 + L_0\dot{p}$$
$$= k_1(s_{1d})\dot{x}_{1d} - k_1(s_1)x_2 + L_0\varepsilon_1. \qquad (15)$$

An inertial filter is used to create virtual control input in (15):

$$\dot{z} = -C(z - s_2), \qquad C > 0,$$
$$z(0) = s_2(0), \qquad \rho := s_2 - z. \qquad (16)$$

That is if the filter transition state is over $z \approx s_2$ and the gap ρ may be arbitrarily narrowed by a proper choice of the filter parameter C $\left(\text{if } |\dot{s}_2| \le c < \infty \text{ then } |\rho| \le \dfrac{c}{C} \text{ [23]} \right)$. Therefore, it is assumed that $|\rho| \le \rho_{\max} < \infty$.

Signals z and s_2 are added and subtracted in (15), the desired trajectory for s_2 is denoted by s_{2d} and the tracking error by:

$$\varepsilon_2 := s_{2d} - s_2. \qquad (17)$$

All these operations transform (15) into the following form:

$$\dot{\varepsilon}_0 = k_1(s_{1d})\dot{x}_{1d} - k_1(s_1)x_2 + L_0\varepsilon_1 - s_{2d} + \varepsilon_2 + z + \rho. \qquad (18)$$

The Lyapunov function for this stage of backstepping is:

$$V_1 = V_0 + \frac{1}{2}\varepsilon_0^2 \qquad (19)$$

hence, the Lyapunov function derivative takes the following form:

$$\dot{V}_1 = -L_0 p^2 + \varepsilon_0 (k_1(s_{1d})\dot{x}_{1d} - k_1(s_1)x_2)$$
$$+ \varepsilon_0 (z + p + L_0\varepsilon_1 - s_{2d} + \varepsilon_2 + \rho). \qquad (20)$$

Therefore, selecting the reference s_{2d} as:

$$s_{2d} = k_1(s_{1d})\dot{x}_{1d} - k_1(s_1)x_2 + z + p + L_0\varepsilon_1 + L_1\varepsilon_0 \qquad (21)$$

reduces the expression (20) to a simple form:

$$\dot{V}_1 = -L_0 p^2 - L_1\varepsilon_0^2 + \varepsilon_0\varepsilon_2 + \varepsilon_0\rho \qquad (22)$$

and transforms the error dynamics description (18) into:

$$\dot{\varepsilon}_0 = -L_1\varepsilon_0 - p + \varepsilon_2 + \rho = -L_1\varepsilon_0 - p + s_{2d} - z. \qquad (23)$$

The derivative of the reference s_{2d} is calculated as:

$$\dot{s}_{2d} = \frac{d}{dt} [k_1(s_{1d})\dot{x}_{1d} - k_1(s_1)x_2]$$
$$+ \frac{d}{dt} [z + L_0\varepsilon_1 + L_1\varepsilon_0 + p]$$
$$= (h_1(s_{1d})k_1(s_{1d})\dot{x}_{1d})\dot{x}_{1d} + k_1(s_{1d})\ddot{x}_{1d}$$
$$- h_1(s_1)k_1(s_1)\dot{x}_1 x_2 - k_1(s_1)\dot{x}_2$$
$$- C(z - s_2) + \dot{p} + L_0\dot{\varepsilon}_1 + L_1\dot{\varepsilon}_0 \qquad (24)$$

and may be simplified by plugging in expressions for $\dot{x}_1$, $\dot{x}_2$, $\dot{\varepsilon}_1$, $\dot{\varepsilon}_0$. Following these substitutions, $\dot{s}_{2d}$ is represented in a compact form:

$$\dot{s}_{2d} = G - \frac{k_1(s_1)}{J} (\theta^T \xi + gu), \qquad (25)$$

where

$$G := h_1(s_{1d})k_1(s_{1d})\dot{x}_{1d}^2 + k_1(s_{1d})\ddot{x}_{1d}$$
$$- h_1(s_1)k_1(s_1)x_2^2 + \varepsilon_1 - L_0 L_1\varepsilon_0$$
$$- L_0 p + L_0 (s_{2d} - z) - L_0^2\varepsilon_1 - L_1^2\varepsilon_0$$
$$- L_1 p - C(z - s_2) - L_1 [z - s_{2d}]. \qquad (26)$$

Step 2:

Finally, tracking error ε_2 is considered:

$$\dot{\varepsilon}_2 = \frac{d}{dt}(s_{2d} - s_2) = G - k_2(s_2)\dot{x}_2 - \frac{k_1(s_1)}{J}(\theta^T\xi + gu)$$
$$= G - \frac{k_1(s_1)}{J}(\theta^T\xi + gu) - \frac{k_2(s_2)}{J}(\theta^T\xi + gu)$$
$$= G - \frac{[k_1(s_1) + k_2(s_2)]}{J}(\theta^T\xi + gu). \qquad (27)$$

It may be represented in a linear-in-parameters form:

$$\frac{J}{g}\dot{\varepsilon}_2 = \frac{J}{g}G - [k_1(s_1) + k_2(s_2)]\left(\frac{1}{g}\theta^T\xi + u\right)$$
$$= \vartheta^T\varphi - [k_1(s_1) + k_2(s_2)]u, \qquad (28)$$

where

$$\vartheta^T := \begin{bmatrix} \dfrac{J}{g} & \dfrac{1}{g}\theta^T \end{bmatrix},$$

$$\varphi := \begin{bmatrix} G \\ -[k_1(s_1) + k_2(s_2)]\xi \end{bmatrix} \qquad (29)$$

are unknown constant parameters and a known regressor, respectively. The unknown parameters will be substituted by adaptive parameters $\hat{\vartheta}$ and the error of adaptation is denoted by $\tilde{\vartheta} := \vartheta - \hat{\vartheta}$.

The final Lyapunov function is then:

$$V_2 = V_1 + \frac{1}{2}\frac{J}{g}\varepsilon_2^2 + \frac{1}{2}\tilde{\vartheta}^T\Gamma^{-1}\tilde{\vartheta} \qquad (30)$$

J. Kabziński and P. Mosiołek

(with a positive definite matrix Γ), and so:

$$\dot{V}_2 = -L_0 p^2 - L_1 \varepsilon_0^2 + \varepsilon_0 \varepsilon_2 + \varepsilon_0 \rho$$
$$+ \varepsilon_2 \left(\vartheta^T \varphi - [k_1(s_1) + k_2(s_2)] u \right) + \tilde{\vartheta}^T \Gamma^{-1} \frac{d}{dt} \tilde{\vartheta}. \quad (31)$$

The control is as follows:

$$u = \frac{1}{k_1(s_1) + k_2(s_2)} \left(\hat{\vartheta}^T \varphi + L_2 \varepsilon_2 + \varepsilon_0 \right), \quad (32)$$

where $L_2 > 0$ and the identity $\frac{d}{dt} \tilde{\vartheta} = -\frac{d}{dt} \hat{\vartheta}$, reduce (29) to:

$$\dot{V}_2 = -L_0 p^2 - L_1 \varepsilon_0^2 - L_2 \varepsilon_2^2 + \varepsilon_0 \rho$$
$$+ \tilde{\vartheta}^T \left(\varepsilon_2 \varphi - \Gamma^{-1} \frac{d}{dt} \hat{\vartheta} \right). \quad (33)$$

If the robust adaptive law

$$\frac{d}{dt} \hat{\vartheta} = \Gamma \left(\varepsilon_2 \varphi - \sigma \|e\| \hat{\vartheta} \right) \sigma > 0,$$
$$e = \begin{bmatrix} p, & \varepsilon_0, & \varepsilon_2 \end{bmatrix}^T \quad (34)$$

is applied, the well-known inequality $\tilde{\vartheta}^T \hat{\vartheta} \leq \|\tilde{\vartheta}\| (\|\vartheta\| - \|\tilde{\vartheta}\|)$ and the notation of $L_{\min} = \min\{L_0, L_1, L_2\}$ allows to simplify the Lyapunov function derivative:

$$\dot{V}_2 \leq -\|e\| \left\{ L_{\min} \|e\| - \sigma \|\tilde{\vartheta}\| (\|\vartheta\| - \|\tilde{\vartheta}\|) - \rho_{\max} \right\}. \quad (35)$$

Therefore, if $\|\vartheta\| < \|\tilde{\vartheta}\|$ then $-\sigma \|\tilde{\vartheta}\| (\|\vartheta\| - \|\tilde{\vartheta}\|) > 0$ and so, $\dot{V}_2 \leq 0$ for any $\|e\| > \dfrac{\rho_{\max}}{L_{\min}}$. If $\|\vartheta\| > \|\tilde{\vartheta}\|$ then $0 < \|\tilde{\vartheta}\| (\|\vartheta\| - \|\tilde{\vartheta}\|) \leq \dfrac{\|\vartheta\|^2}{4}$ and hence, $\dot{V}_2 \leq 0$ for any $\|e\| > \dfrac{\rho_{\max} + \sigma \dfrac{\|\vartheta\|^2}{4}}{L_{\min}}$.

The derivation of the controller may be summarized by the corollary which follows from the Lyapunov theorem extensions [24]:

Corollary 1. Under the proposed control, the adaptive parameter errors $\tilde{\vartheta}$ and the tracking errors $e = \begin{bmatrix} p, & \varepsilon_0, & \varepsilon_2 \end{bmatrix}^T$ are uniformly ultimately bounded (UUB). Increasing the design parameter $L_{\min}$ allows to reduce the limit set for e freely.

As the state variables p, ε_0, ε_2 are UUB, so is $\varepsilon_1 = \varepsilon_0 - L_0 p$ and the design parameter $L_{\min}$ may be used to narrow the tracking error.

It follows (from the boundedness of the error variables, under the assumption that the desired trajectory x_{1d}, $\dot{x}_{1d}$ stays inside constraints (2)) that the state variables s_1 and s_2 are bounded, and hence x_1 and x_2 stay inside constraints (2).

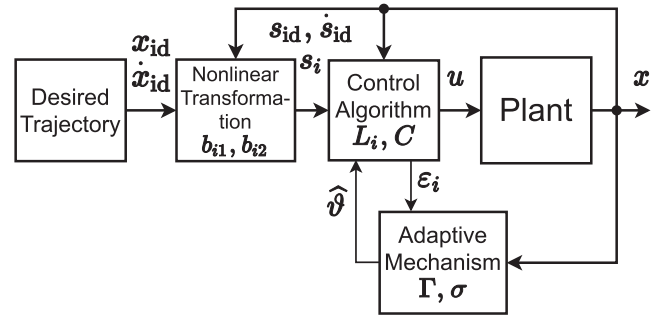The final scheme of the control system is presented in Fig. 2.

Fig. 2. Control system scheme with design parameters

5. Switching the integrator off

The integrator applied in the derived control scheme helps reduce tracking errors caused mostly by inaccurate compensation and filter error ρ, which may be considered an external disturbance. However, the simplified controller without the integrator will also assure closed-loop system stability in the UUB sense. It is obviously not recommended to switch the integrator off or on during the system transient, but the same control structure may be started with or without the integrator.

If the integrator is switched off by taking $L_0 = 0$, variable p is not used by the controller. In the signal: $\varepsilon_{1d} = -L_0 p = 0$, and $\varepsilon_0 = \varepsilon_1$ (see Fig. 3). The derivation starts with dynamics of ε_1 in (10) and is summarized in the following formulae:

$$\dot{\varepsilon}_1 = k_1(s_{1d}) \dot{x}_{1d} - k_1(s_1) x_2 - s_{2d} + \varepsilon_2 + \rho, \quad (36)$$

$$s_{2d} = [k_1(s_{1d}) \dot{x}_{1d} - k_1(s_1) x_2 + z] + L_1 \varepsilon_1, \quad (37)$$

$$\dot{s}_{2d} = G - \frac{k_1(s_1)}{J} \left(\theta^T \xi + g u \right), \quad (38)$$

$$G := h_1(s_{1d}) k_1(s_{1d}) \dot{x}_{1d}^2$$
$$+ k_1(s_{1d}) \ddot{x}_{1d} - h_1(s_1) k_1(s_1) x_2^2$$
$$- L_1^2 \varepsilon_1 - C(z - s_2) - L_1 [z - s_{2d}], \quad (39)$$

$$V_2 = \frac{1}{2} \varepsilon_1^2 + \frac{1}{2} \frac{J}{g} \varepsilon_2^2 + \frac{1}{2} \tilde{\vartheta}^T \Gamma^{-1} \tilde{\vartheta}, \quad (40)$$

$$u = \frac{1}{k_1(s_1) + k_2(s_2)} \left(\hat{\vartheta}^T \varphi + L_2 \varepsilon_2 + \varepsilon_1 \right), \quad (41)$$

$$\frac{d}{dt} \hat{\vartheta} = \Gamma \left(\varepsilon_2 \varphi - \sigma \|e\| \hat{\vartheta} \right),$$
$$\sigma > 0, \qquad e = \begin{bmatrix} \varepsilon_1, & \varepsilon_2 \end{bmatrix}^T. \quad (42)$$

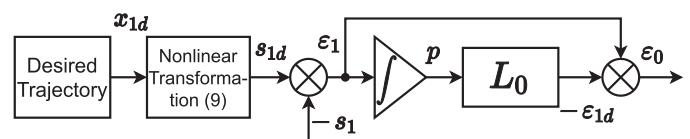The conclusions about UUB stability are similar, with $L_{\min} = \min\{L_1, L_2\}$.

Fig. 3. Integrator loop scheme

6. Example

Both controllers (with and without the integrator) were tested for the permanent magnet synchronous motor drive, propelling the stiff arm working against the gravitational force. The current control loop assures that direct axis current i_d is close to zero and that torque is proportional to the desired value u of the quadrature axis current i_q The plant model is described by the following equations:

$$\dot{x}_1 = x_2,$$
$$J\dot{x}_2 = -bx_2 + c\sin(x_1) - T_f(x_2) + k_i u. \tag{43}$$

Friction torque T_f is given by:

$$T_f = a_1 (\tanh(a_2 x_2) - \tanh(a_3 x_2)) + a_4 \tanh(a_5 x_2). \tag{44}$$

Such smooth model of friction was frequently used in the literature – see [25, 26] for details. According to the previous notation:

$$\xi = \begin{bmatrix} -x_2 \\ \sin(x_1) \\ -\tanh(a_2 x_2) + \tanh(a_3 x_2) \\ -\tanh(a_5 x_2) \end{bmatrix} \tag{45}$$

and the adaptive parameters θ^T correspond to the unknown $[b, c, a_1, a_4]$. The nominal values of parameters are $J = 0.1$ [kgm^2], $b = 0.3$ $\left[\text{Nm}\dfrac{\text{s}}{\text{rad}}\right]$, $c = 2$, $a_1 = 40$ [Nm], $a_2 = 110$, $a_3 = 100$, $a_4 = 2$, $a_5 = 100$ and $k_i = 2$ $\left[\dfrac{\text{Nm}}{\text{A}}\right]$.

It is assumed that state variables of system (2) must fulfill constraints $b_{11} = b_{12} = 1$ [rad] and $b_{21} = b_{22} = 5$ $\left[\dfrac{\text{rad}}{\text{s}}\right]$.

The aim of the first experiment was to stabilize the drive, so $x_{1d} = \dot{x}_{1d} = 0$. The gains selected for all simulations are $L_0 = 15$ or $L_0 = 0$ when the integrator is switched off; $L_1 = 15$, $L_2 = 15$. Figs. 4, 5 show system trajectories corresponding to different initial conditions. The starting values for adaptive parameters equal 80% of their nominal values and $\Gamma = \text{diag}(0.007; 10; 10; 10; 10)$, $\sigma = 0.01$.
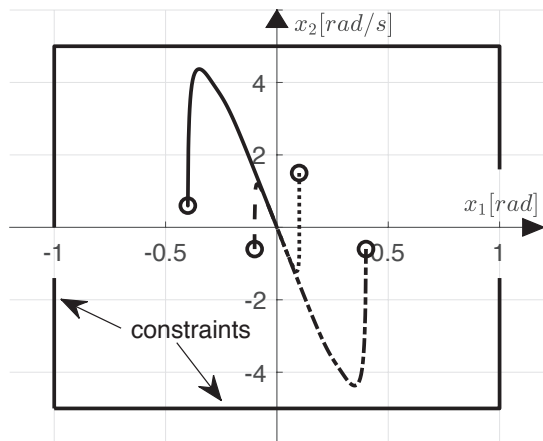
Fig. 4. Trajectories of state variables for several starting points. System without the integrator, "o" – initial conditions
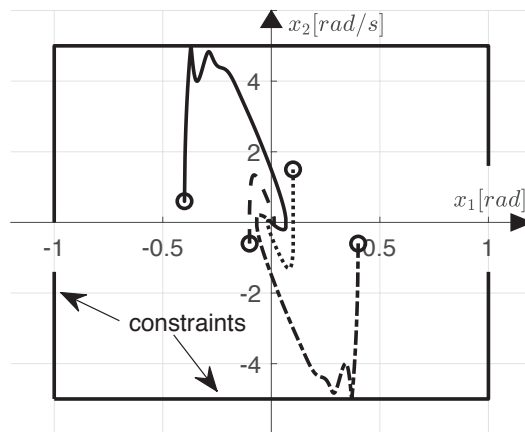
Fig. 5. Trajectories of state variables for several starting points. System with the integrator, "o" – initial conditions

All trajectories for both controllers (Figs. 4, 5) remain in the bounded area. If the integrator is switched on, the speed is closer to the constraint and more oscillations are visible in Fig. 5. Next, the influence of the control gains L_0, L_1, L_2 was demonstrated. The state variables for different values of parameters L_i are shown in Figs. 6, 7.
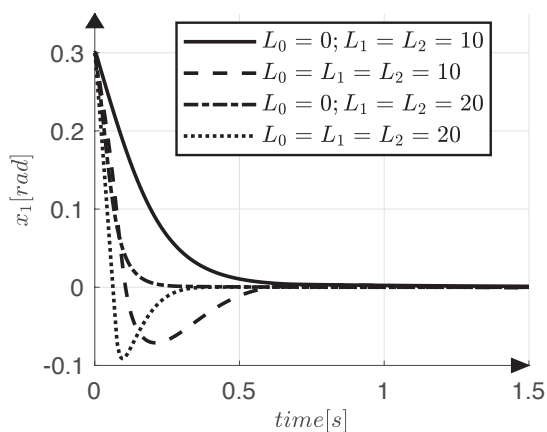
Fig. 6. Stabilization of position x_1 for different values of L_1 and L_2. If $L_0 = 0$, the integrator is off, if $L_0 > 0$, it is on
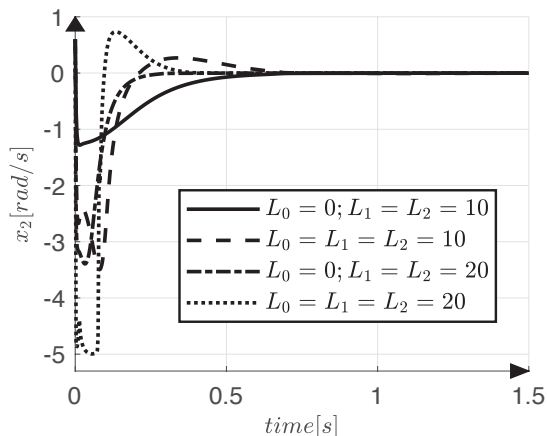
Fig. 7. Stabilization of velocity x_2 for different values of L_1 and L_2. If $L_0 = 0$, the integrator is off, if $L_0 > 0$, it is on

The aim of the second experiment was to follow the desired trajectory $x_{1d} = 0.\overline{9}\sin(0.25t)$ under the constraints $b_{11} = b_{12} = 1$ and $b_{21} = b_{22} = 5$.

The control system includes the model of a PMSM motor

$$L_d \frac{\mathrm{d}}{\mathrm{d}t} i_d = -Ri_d + \omega_e L_q i_q + u_d\,,$$
$$L_q \frac{\mathrm{d}}{\mathrm{d}t} i_q = -Ri_q - \omega_e (L_d i_d + \varphi_m) + u_q\,, \qquad (46)$$
$$T = k_i i_q\,,$$

with parameters from Table 1.

Table 1
Motor parameters and signals

L_d	d-axis inductance	8.7 [mH]
L_q	q-axis inductance	8.7 [mH]
R	phase resistance	1.71 [Ω]
φ_m	permanent magnet flux	0.86 [Vs/rad]
k_i	torque constant	2 [Nm/A]
i_d, i_q	d- and q-axis currents	6.5 [A]
ω_e	electric velocity	1500 [rot./min]
u_d, u_q	d- and q-axis voltages	400 [V]
T	motor torque	13 [Nm]

Linearizing control $u_q = \omega_e (L_d i_d + \varphi_m) + v_q$ allows for simplifying the current control design – we are to select a PI controller $C(s) = K_q \left(1 + \dfrac{1}{sT_{iq}}\right)$ for an inertial plant $P(s) = \dfrac{1}{sL_q + R}$. This was done by means of standard linear control techniques. The PI controller was tuned to make the i_q dominant time constant $\sim 100\ \mu s$.

The current generation dynamics

$$u = i_q = \frac{K_q \left(1 + \dfrac{1}{sT_{iq}}\right) \dfrac{1}{sL_q + R}}{1 + K_q \left(1 + \dfrac{1}{sT_{iq}}\right) \dfrac{1}{sL_q + R}} u_0$$

obtained were included between the output of the nonlinear, adaptive controller u_0 and the input of the system (43) u.

The tracking errors for both controllers are shown in Fig. 8, 9. Both controllers provide sufficient accuracy of tracking. The integrator allows for reducing the quasi-steady-state error by 20% approximately.

The motor current is plotted out in Fig. 10. Integrator results are used for more aggressive control of the initial state (initial current peek). This may be reduced by the proper parameter tuning as is demonstrated by the third experiment, below.

The norm of the error of adaptive parameters is presented in Fig. 11. For both controllers, the adaptive parameters remain
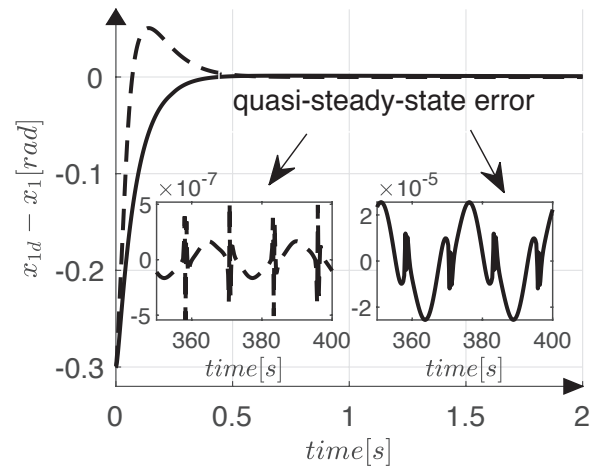

Fig. 8. Tracking error $x_{1d} - x_1$ for both controllers: dashed line – controller with the integrator, solid line – controller without the integrator
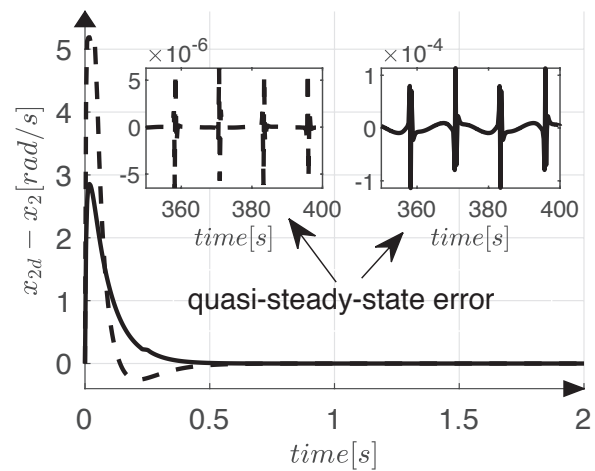

Fig. 9. Tracking error $x_{2d} - x_2$ for both controllers: dashed line – controller with the integrator, solid line – controller without the integrator

bounded, as has been proven, and the rate of change of adaptive parameters is moderate, facilitating practical applications.
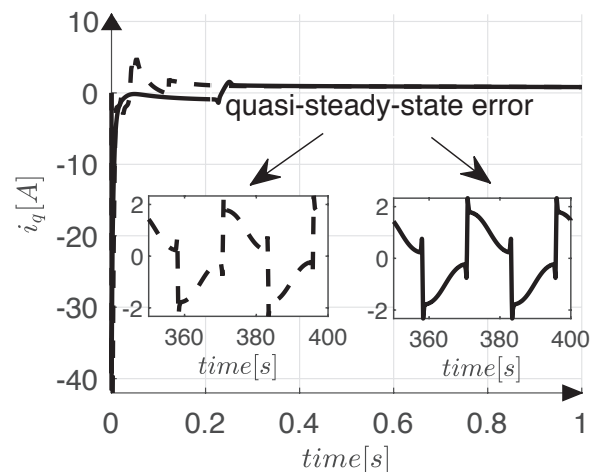

Fig. 10. Current i_q for both controllers: dashed line – controller with the integrator, solid line – controller without the integrator
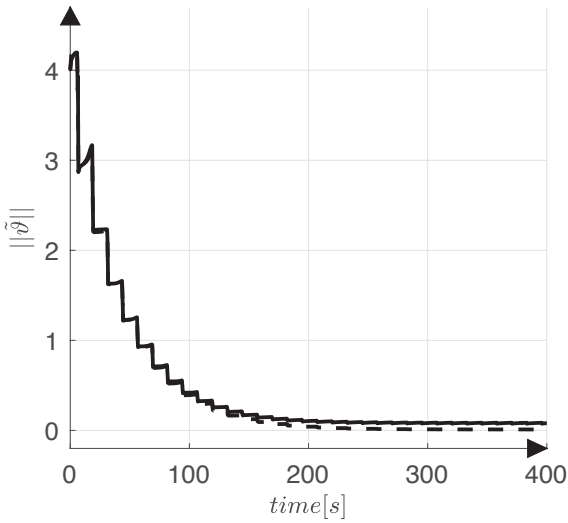
Fig. 11. Norm of the error of adaptive parameters $\left\| \tilde{\vartheta} \right\|$ for both controllers: dashed line – controller with the integrator, solid line – controller without the integrator

Evidence that the velocity constraint is active and truly influences system performance is presented in Fig. 12. If the constraint is not imposed ($b_{21} = b_{22} = \infty$), maximum value of motor velocity during the transient is $\sim 4.3 \left[\dfrac{\text{rad}}{\text{s}} \right]$, while when $b_{21} = b_{22} = 3$ the velocity constraint is strictly preserved.

Fig. 12. Velocity x_2 for the controller with the integrator: solid line – constraint $b_{21} = b_{22} = 3$, dashed line – controller without velocity constraints

The effect of active velocity constraints on the tracking errors is presented in Figs. 13, 14. Only the initial part of the time-history is affected. Convergence is slightly slower when the constraints are active, but the velocity overshoot and the motor current are actually significantly smaller (Fig. 15).

The aim of the third experiment was to demonstrate the influence of design parameters L_i and velocity constraints b_{21} and
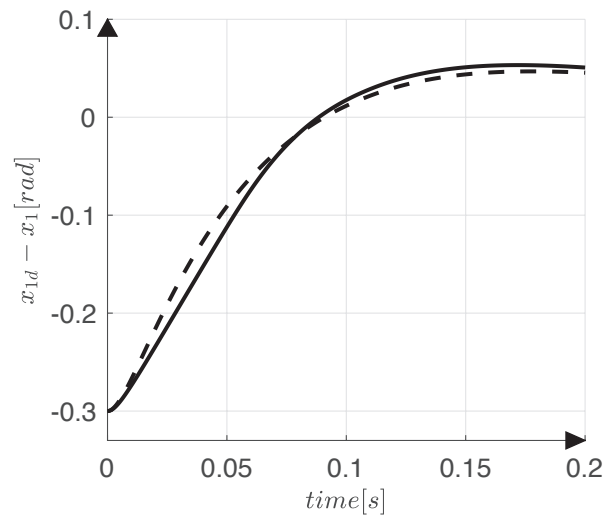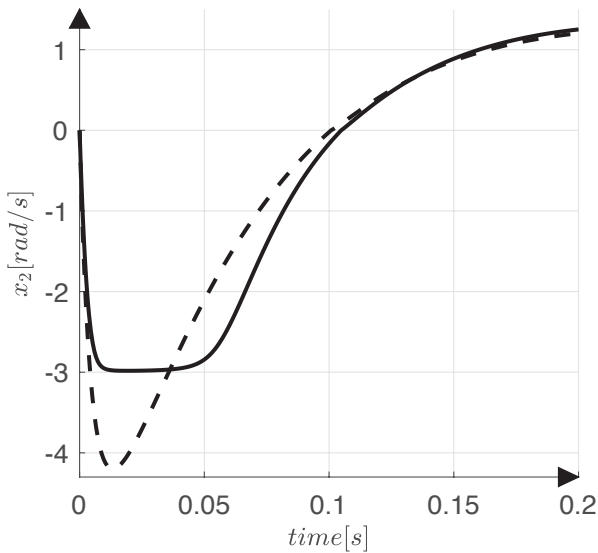

Fig. 13. Tracking error $x_{1d} - x_1$ for the controller with the integrator: solid line – constraint $b_{21} = b_{22} = 3$, dashed line – controller without velocity constraints
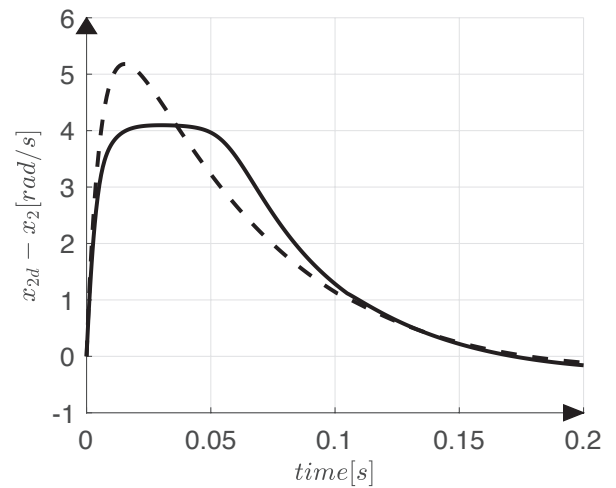

Fig. 14. Tracking error $\dot{x}_{1d} - x_2 := x_{2d} - x_2$ for the controller with the integrator: solid line – constraint $b_{21} = b_{22} = 3$, dashed line – controller without velocity constraints
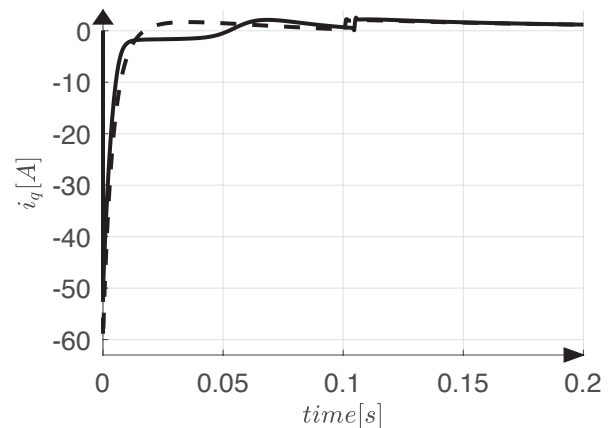

Fig. 15. Current i_q for the controller with the integrator: solid line – constraint $b_{21} = b_{22} = 3$, dashed line – controller without velocity constraints

b_{22} on the maximum value I_m of current i_q during the transient response. The desired trajectory and the position constraint are the same as previously. The results obtained are presented in Tables 2 and 3.

Table 2
I_m value for different velocity constraints ($L_i = 10$)

Velocity constraints $b_{21} = b_{22}$	I_m [A] Controller with integrator	I_m [A] Controller without integrator
2.3	43.5	22.0
2.5	44.0	22.5
3.0	46.0	23.5
5.0	50.5	25.5

Table 3
I_m value for different value of parameters L_i ($b_{21} = b_{22} = 3$)

Parameters L_i	I_m [A] Controller with integrator	I_m [A] Controller without integrator
8	30.0	16.0
10	46.0	23.5
12	65.5	33.0

Increasing parameters b_{21} and L_i increases maximum current value I_m. The presence or absence of the integrator in the controller has the largest influence on the value of I_m.

7. Conclusions

An adaptive control problem with hard state constraints was formulated and solved for a servo drive. The proposed approach was based on adaptive backstepping and nonlinear state transformation. This allows us to impose hard constraints on the state variables directly and to eliminate the restrictive feasibility conditions, imposed by the BLF approach.

Two adaptive nonlinear controllers were proposed. Both control algorithms are sufficiently accurate from a practical point of view. The adaptive structure guaranties proven robustness against parametric model uncertainties. The technique presented allows for obtaining rigorous proof of closed loop system stability in the UUB sense. The controllers derived are not difficult to tune and the approach proposed can be easily extended to time varying-constraints. The experiments performed demonstrate that both controllers are robust against un-modeled dynamics of the plant.

The controller with an integrator allows for further reduction of the tracking error, especially during quasi-steady-state operation. Unfortunately, the integrator gain, which reduces the quasi-steady-state tracking error, results in more aggressive control during the initial part of the transient response, with a high peek of the motor current. Therefore, the adaptive approach to the integrator gain will be investigated in the next contribution.

References

[1] F. Blanchini, "Set invariance in control", *Automatica* 35(11) 1747–1767 (1999).

[2] E. Pérez, C. Ariño, F.X. Blasco, and M.A. Martínez, "Maximal closed loop admissible set for linear systems with non-convex polyhedral constraints", *J. Process Control* 21(4), 529–537 (2011).

[3] E.G. Gilbert and K.T. Tan, "Linear systems with state and control constraints: the theory and application of maximal output admissible sets", *IEEE Trans. Automat. Contr.* 36(9), 1008–1020 (1991).

[4] R. Wang and J. Bao, "A differential Lyapunov-based tube MPC approach for continuous-time nonlinear processes", *J. Process Control* 83, 155–163 (2019).

[5] D.Q. Mayne, J.B. Rawlings, C.V. Rao, and P.O.M. Scokaert, "Constrained model predictive control: stability and optimality", *Automatica* 36(6), 789–814 (2000).

[6] K. Kogiso and K. Hirata, "Reference governor for constrained systems with time-varying references", *Rob. Auton Syst.* 57(3), 289–295 (2009).

[7] S. Oh-hara, Y. Urano, and F. Matsuno, "The control of constrained system with time-delay and its experimental evaluations using RC model helicopter", in *2007 International Conference on Control, Automation and Systems*, 2007, pp. 2897–2901.

[8] J. Li and Y. Liu, "Control of nonlinear systems with full state constraints using integral Barrier Lyapunov Functionals", in *2015 International Conference on Informative and Cybernetics for Computational Social Systems (ICCSS)*, 2015, pp. 66–71.

[9] W. Wang and S. Tong, "Adaptive fuzzy containment control of nonlinear strict-feedback systems with full state constraints", *IEEE Trans. Fuzzy Syst.* 27(10), 2024–2038 (2019).

[10] K. Sachan and R. Padhi, "Output-constrained robust adaptive control for uncertain nonlinear MIMO systems with unknown control directions", *IEEE Control Syst. Lett.* 3(4), 823–828 (2019).

[11] S. Luo and Y. Song, "Chaos analysis-based adaptive backstepping control of the microelectromechanical resonators with constrained output and uncertain time delay", *IEEE Trans. Ind. Electron.* 63(10), 6217–6225 (2016).

[12] C. Wang, Y. Wu, and J. Yu, "Barrier Lyapunov functions-based adaptive control for nonlinear pure-feedback systems with time-varying full state constraints", *Int. J. Control. Autom. Syst.* 15(6), 2714–2722 (2017).

[13] C. Wang, Y. Wu, F. Wang, and Y. Zhao, "TABLF-based adaptive control for uncertain nonlinear systems with time-varying asymmetric full-state constraints", *Int. J. Control* (2019), doi: 10.1080/00207179.2019.1639825.

[14] Z. Yin, B. Wang, C. Du, and Y. Zhang, "Barrier-Lyapunov-function-based backstepping control for PMSM servo system with full state constraints", in *2019 22nd International Conference on Electrical Machines and Systems (ICEMS)*, 2019, pp. 1–5.

[15] J. Kabziński, P. Mosiołek, and M. Jastrzębski, "Adaptive position tracking with hard constraints – barrier Lyapunov functions approach", in *Studies in Systems, Decision and Control*, vol. 75, Springer Berlin Heidelberg, pp. 27–52, 2017.

[16] Z.L. Tang, S.S. Ge, K.P. Tee, and W. He, "Robust adaptive neural tracking control for a class of perturbed uncertain nonlinear systems with state constraints", *IEEE Trans. Syst. Man, Cybern. Syst.* 46(12), 1618–1629 (2016).

[17] K.P. Tee and S.S. Ge, "Control of nonlinear systems with partial state constraints using a barrier Lyapunov function", *Int. J. Control.* 84(12), 2008–2023 (2011).

[18] J. Kabziński, "Adaptive, compensating control of wheel slip in railway vehicles", *Bull. Pol. Ac.: Tech.* 63(4), 955–963 (2015).

[19] P. Serkies, "A novel predictive fuzzy adaptive controller for a two-mass drive system", *Bull. Pol. Ac.: Tech.* 66(1), 37–47 (2018).

[20] T. Białoń, M. Pasko, A. Lewicki, and R. Niestrój, "Parameter selection of an adaptive PI state observer for an induction motor", *Bull. Pol. Ac.: Tech.* 61(3), 599–603 (2013).

[21] T. Orlowska-Kowalska and M. Dybkowski, "Performance analysis of the sensorless adaptive sliding-mode neuro-fuzzy control of the induction motor drive with MRAS-type speed estimator", *Bull. Pol. Ac.: Tech.* 60(1), 61–70 (2012).

[22] M. Krstic, K. Ioannis, and P.V. Kokotovic, *Nonlinear and Adaptive Control Design*, Wiley, 1995.

[23] J. Kabziński and P. Mosiołek, *Projektowanie nieliniowych układów sterowania (Nonlinear Control Design)*, Wydawnictwo Naukowe PWN, 2018.

[24] H.K. Khalil, *Nonlinear Systems*, Prentice Hall, 2000

[25] C. Makkar, G. Hu, W.G. Sawyer, and W.E. Dixon, "Lyapunov-Based Tracking Control in the Presence of Uncertain Nonlinear Parameterizable Friction", *IEEE Trans. Automat. Contr.* 52(10), 1988–1994 (2007).

[26] Y. Zhang, S. Li, X. Luo, and M. Shang, "A dynamic neural controller for adaptive optimal control of permanent magnet DC motors, in *2017 International Joint Conference on Neural Networks (IJCNN)*, 2017, pp. 839–844.